

Uncertainty in Model-Agnostic Meta-Learning using Variational Inference

Cuong Nguyen
University of Adelaide

cuong.nguyen@adelaide.edu.au

Thanh-Toan Do
University of Liverpool

thanh-toan.do@liverpool.ac.uk

Gustavo Carneiro
University of Adelaide

gustavo.carneiro@adelaide.edu.au

Abstract

We introduce a new, rigorously-formulated Bayesian meta-learning algorithm that learns a probability distribution of model parameter prior for few-shot learning. The proposed algorithm employs a gradient-based variational inference to infer the posterior of model parameters to a new task. Our algorithm can be applied to any model architecture and can be implemented in various machine learning paradigms, including regression and classification. We show that the models trained with our proposed meta-learning algorithm are well calibrated and accurate, with state-of-the-art calibration and classification results on two few-shot classification benchmarks (Omniglot and Mini-ImageNet), and competitive results in a multi-modal task-distribution regression.

1. Introduction

Machine learning, in particular deep learning, has thrived during the last decade, producing results that were previously considered to be infeasible in several areas. For instance, outstanding results have been achieved in speech and image understanding [1–4], and medical image analysis [5]. However, the development of these machine learning methods typically requires a large number of training samples to achieve notable performance. Such requirement contrasts with the human ability of quickly adapting to new learning tasks using few “training” samples. This difference may be due to the fact that humans tend to exploit prior knowledge to facilitate the learning of new tasks, while machine learning algorithms often do not use any prior knowledge (e.g., training from scratch with random initialisation) [6] or rely on weak prior knowledge to learn new tasks (e.g., training from pre-trained models) [7]. This challenge has motivated the design of machine learning methods that can make more effective use of prior knowledge to adapt to

new learning tasks using few training samples [8].

Such methods assume the existence of a latent distribution over classification or regression tasks that share a common structure. This common structure means that solving many tasks can be helpful for solving a new task, sampled from the same task distribution, even if it contains a limited number of training samples. For instance, in *multi-task learning* [9], an agent simultaneously learns the shared representation of many related tasks and a main task that are assumed to come from the same domain. The extra information provided by this multi-task training tends to regularise the main task training, particularly when it contains few training samples. In *domain adaptation* [10, 11], a learner transfers the shared knowledge of many training tasks drawn from one or several source domains to perform well on tasks (with small training sets) drawn from a target domain. *Bayesian learning* [12] has also been explored, where prior knowledge is represented by a probability density function on the parameters of the visual classes’ probability models. In *learning to learn* or *meta-learning* [13, 14], a meta-learner extracts relevant knowledge from many tasks learned in the past to facilitate the learning of new future tasks.

From the methods above, meta-learning currently produces state-of-the-art results in many benchmark few-shot learning datasets [15–22]. Such success can be attributed to the way meta-learning leverages prior knowledge from several training tasks drawn from a latent distribution of tasks, where the objective is to perform well on unseen tasks drawn from the same distribution. However, a critical issue arises with the limited amount of training samples per task combined with the fact that most of these approaches [15, 16, 18, 19, 23] do not try to estimate model uncertainty – this may result in overfitting. This issue has been recently addressed with Laplace approximation to estimate model uncertainty, involving the computationally hard estimation of a high-dimensional covariance matrix [24], and with vari-

ational Bayesian learning [20, 25] containing sub-optimal point estimate of model parameters and inefficient optimisation.

In this work, we propose a new variational Bayesian learning by extending model-agnostic meta-learning (MAML) [19] based on a rigorous formulation that is efficient and does not require any point estimate of model parameters. In particular, compared to MAML [19], our approach explores probability distributions over possible values of meta-parameters, rather than having a fixed value. Learning and prediction using our proposed method are, therefore, more robust due to the perturbation of learnt meta-parameters that coherently explains data variability. Our evaluation shows that the models trained with our proposed meta-learning algorithm is at the same time well calibrated and accurate, with competitive results in terms of Expected Calibration Error (ECE) and Maximum Calibration Error (MCE), while outperforming state-of-the-art methods in some few-shot classification benchmarks (Omniglot and Mini-ImageNet).

2. Related Work

Meta-learning has been studied for a few decades [13, 14, 26], and recently gained renewed attention with the use of deep learning methods. As meta-learning aims at the unique ability of learning how to learn, it has enabled the development of training methods with limited number of training samples, such as few-shot learning. Some notable meta-learning approaches include memory-augmented neural networks [15], deep metric learning [18, 23], learn how to update model parameters [16] and learn good prior using gradient descent update [19]. These approaches have generated some of the most successful meta-learning results, but they lack the ability to estimate model uncertainty. Consequently, their performances may suffer in uncertain environments and real world applications.

Bayesian meta-learning techniques have, therefore, been developed to incorporate uncertainty into model estimation. Among those, MAML-based meta-learning has attracted much of research interest due to the straightforward use of gradient-based optimisation of MAML. Grant et al. [24] use Laplace approximation to improve the robustness of MAML, but the need to estimate and invert the Hessian matrix makes this approach computationally challenging, particularly for large-scale models, such as the ones used by deep learning methods. Variational inference (VI) addresses such scalability issue – remarkable examples of VI-based methods are PLATIPUS [25], BMAML [20] and the methods similar to our proposal, Amortised meta-learner [27] and VERSA [28]¹. However, PLATIPUS optimises the lower bound of data prediction, leading to the

need to approximate a joint distribution between the task-specific and meta parameters. This approximation complicates the implementation and requires a point estimate of the task-specific parameters to reduce the complexity of the estimation of this joint distribution. Employing point estimate may, however, reduce its ability to estimate model uncertainty. BMAML uses a closed-form solution based on Stein Variational Gradient Descent (SVGD) that simplifies the task adaptation step, but it relies on the use of a kernel matrix, which increases its computational complexity. Amortised meta-learner applies variational approximation on both the meta-parameters and task-specific parameters, resulting in a challenging optimisation. VERSA takes a slightly different approach by employing an external neural network to learn the variational distribution for certain parameters, while keeping other parameters shared across all tasks. Another inference-based method is Neural Process [29] that employs the train-ability of neural networks to model a Gaussian-Process-like distribution over functions to achieve uncertainty quantification in few-shot learning. However, due to the prominent weakness of Gaussian Process that suffers from cubic complexity to data size, this might limit the scalability of Neural Process and makes it infeasible for large-scale datasets.

Our approach, in contrast, employs a straightforward variational approximation for the distribution of only the task-specific parameters, where we do not require the use of point estimate of any term, nor do we need to compute Hessian or kernel matrices or depend on an external network. Our proposed algorithm can be considered a rigorous and computationally efficient Bayesian meta-learning algorithm. A noteworthy non-meta-learning method that employs Bayesian methods is the neural statistician [30] that uses an extra variable to model data distribution within each task, and combines that information to solve few-shot learning problems. Our proposed algorithm, instead, does not introduce additional parameters, while still being able to extract relevant information from a small number of examples.

Our method is also related to deep neural networks initialisation methods. Many previous works have explored various initialisation techniques, such as random [31, 32], data-dependent [33, 34] and learnt initialisers [35, 36]. In contrast, our work is based on empirical Bayesian approaches that learn the distribution of initial model parameters on a given task distribution, and therefore, allows an efficient and robust adaptation for problems such as few-shot learning, where only one or a few gradient steps are performed.

3. Methodology

In this section, we first define and formulate the few-shot meta-learning problem. We then describe MAML, derive our proposed algorithm, and mention the similarities

¹Amortised meta-learner [27] and VERSA [28] have been developed in parallel to our proposed VAMPIRE.

and differences between our method and recently proposed meta-learning methods that are relevant to our proposal.

3.1. Few-shot Learning

While conventional machine learning paradigm is designed to optimise the performance on a single task, few-shot learning is trained on a set of conditional independent and identically distributed (i.i.d.) tasks given meta-parameters. The notation of “task environment” was formulated in [37], where tasks are sampled from an unknown task distribution \mathcal{D} over a family of tasks. Each task \mathcal{T}_i in this family is indexed by $i \in \{1, \dots, T\}$ and consists of a support set $\{\mathcal{X}_i^{(t)}, \mathcal{Y}_i^{(t)}\}$ and a query set $\{\mathcal{X}_i^{(v)}, \mathcal{Y}_i^{(v)}\}$, with $\mathcal{X}_i^{(t)} = \{\mathbf{x}_{ij}^{(t)}\}_{j=1}^M$ and $\mathcal{Y}_i^{(t)} = \{y_{ij}^{(t)}\}_{j=1}^M$ ($\mathcal{X}_i^{(v)}$ and $\mathcal{Y}_i^{(v)}$ are similarly defined). The aim of few-shot learning is to predict the output $y_{ij}^{(v)}$ of the query input $\mathbf{x}_{ij}^{(v)}$ given the small support set for task \mathcal{T}_i ($M \leq 20$). Similarly to recent methods based on MAML [24], we rely on a Bayesian hierarchical model as shown in Figure 1a, where θ denotes the meta parameters, and \mathbf{w}_i represents the task-specific parameters for task \mathcal{T}_i . In [19], \mathbf{w}_i are the neural network weights for task \mathcal{T}_i obtained by performing truncated gradient descent using $\mathcal{X}_i^{(t)}$ and $\mathcal{Y}_i^{(t)}$ from the initial weight values θ .

The objective function of few-shot learning is, therefore, to find a meta-learner, parameterised by θ , across tasks sampled from \mathcal{D} , as follows:

$$\theta^* = \arg \min_{\theta} -\log p(\mathcal{Y}_{1:T}^{(v)} | \mathcal{Y}_{1:T}^{(t)}, \theta) \quad (1)$$

where T denotes the number of tasks, and, hereafter, we simplify the notation by dropping the explicit dependence on $\mathcal{X}_i^{(t)}$ and $\mathcal{X}_i^{(v)}$ from the set of conditioning variables. The likelihood term on the right hand side of (1) can be rewritten in the logarithm form and expanded by applying the sum rule of probability:

$$\begin{aligned} -\log p(\mathcal{Y}_{1:T}^{(v)} | \mathcal{Y}_{1:T}^{(t)}, \theta) &= \sum_{i=1}^T -\log p(\mathcal{Y}_i^{(v)} | \mathcal{Y}_i^{(t)}, \theta) \\ &= \sum_{i=1}^T -\log \mathbb{E}_{p(\mathbf{w}_i | \mathcal{Y}_i^{(t)}, \theta)} \left[p(\mathcal{Y}_i^{(v)} | \mathbf{w}_i) \right]. \end{aligned} \quad (2)$$

The negative log-likelihood in (2) can be simplified with Jensen’s inequality to obtain an upper bound:

$$\mathcal{L}^{(v)}(\theta) = \sum_{i=1}^T -\mathbb{E}_{p(\mathbf{w}_i | \mathcal{Y}_i^{(t)}, \theta)} \left[\log p(\mathcal{Y}_i^{(v)} | \mathbf{w}_i) \right]. \quad (3)$$

Hence, instead of minimising the negative log-likelihood in (1), we minimise the upper bound of the corresponding negative log-likelihood presented in (3). If the distribution of task-specific posterior, $p(\mathbf{w}_i | \mathcal{Y}_i^{(t)}, \theta)$, is well-behaved, we can apply Monte Carlo to approximate the

expectation in (3) by sampling model parameters \mathbf{w}_i from $p(\mathbf{w}_i | \mathcal{Y}_i^{(t)}, \theta)$. Thus, depending on the formulation of the posterior $p(\mathbf{w}_i | \mathcal{Y}_i^{(t)}, \theta)$, we can formulate different algorithms to solve the problem of few-shot learning. The following subsections present different methods to approximate that posterior to minimise (3).

3.2. Point Estimate - MAML

A simple way is to approximate the posterior $p(\mathbf{w}_i | \mathcal{Y}_i^{(t)}, \theta)$ by a Dirac Delta function at its local mode:

$$p(\mathbf{w}_i | \mathcal{Y}_i^{(t)}, \theta) = \delta(\mathbf{w}_i - \mathbf{w}_i^{\text{MAP}}), \quad (4)$$

where the local mode $\mathbf{w}_i^{\text{MAP}}$ can be obtained by using maximum a posterior (MAP):

$$\mathbf{w}_i^{\text{MAP}} = \arg \max_{\mathbf{w}_i} \log p(\mathcal{Y}_i^{(t)} | \mathbf{w}_i) + \log p(\mathbf{w}_i; \theta). \quad (5)$$

In the simplest case where the prior is deterministic: $p(\mathbf{w}_i; \theta) = \delta(\mathbf{w}_i - \theta)$, and gradient descent is used, the local mode can be determined as

$$\mathbf{w}_i^{\text{MAP}} = \theta - \alpha \nabla_{\mathbf{w}_i} \left[-\log p(\mathcal{Y}_i^{(t)} | \mathbf{w}_i) \right], \quad (6)$$

where α is the learning rate, and the truncated gradient descent consists of a single step of (6) (the extension to a larger number of steps is trivial). Given the point estimate assumption in (4), the upper bound of the negative log-likelihood in (3) can be presented as:

$$\mathcal{L}^{(v)}(\theta) = \sum_{i=1}^T -\log p(\mathcal{Y}_i^{(v)} | \mathbf{w}_i^{\text{MAP}}). \quad (7)$$

Minimising the upper bound of the negative log-likelihood in (7) with respect to the meta parameters θ represents the MAML algorithm [19]. This derivation also explains the intuition behind MAML, which is to find a good initialisation of model parameters to learn new tasks drawn from \mathcal{D} as illustrated in Figure 1b.

3.3. Gradient-based Variational Inference

In contrast to the method in Sec. 3.2, we approximate the posterior $p(\mathbf{w}_i | \mathcal{Y}_i^{(t)}, \theta)$ with a variational distribution $q(\mathbf{w}_i; \lambda_i)$, parameterized by λ_i , that minimises the Kullback-Leibler (KL) divergence with the true distribution $p(\mathbf{w}_i | \mathcal{Y}_i^{(t)}, \theta)$:

$$\begin{aligned} \lambda_i^* &= \arg \min_{\lambda_i} \text{KL} \left[q(\mathbf{w}_i; \lambda_i) \| p(\mathbf{w}_i | \mathcal{Y}_i^{(t)}, \theta) \right] \\ &= \arg \min_{\lambda_i} \int q(\mathbf{w}_i; \lambda_i) \log \frac{q(\mathbf{w}_i; \lambda_i) p(\mathcal{Y}_i^{(t)} | \theta)}{p(\mathcal{Y}_i^{(t)} | \mathbf{w}_i) p(\mathbf{w}_i; \theta)} d\mathbf{w}_i \\ &= \arg \min_{\lambda_i} \text{KL} [q(\mathbf{w}_i; \lambda_i) \| p(\mathbf{w}_i; \theta)] \\ &\quad - \mathbb{E}_{q(\mathbf{w}_i; \lambda_i)} \left[\log p(\mathcal{Y}_i^{(t)} | \mathbf{w}_i) \right] + \underbrace{\log p(\mathcal{Y}_i^{(t)} | \theta)}_{\text{const. wrt } \lambda_i}. \end{aligned} \quad (8)$$

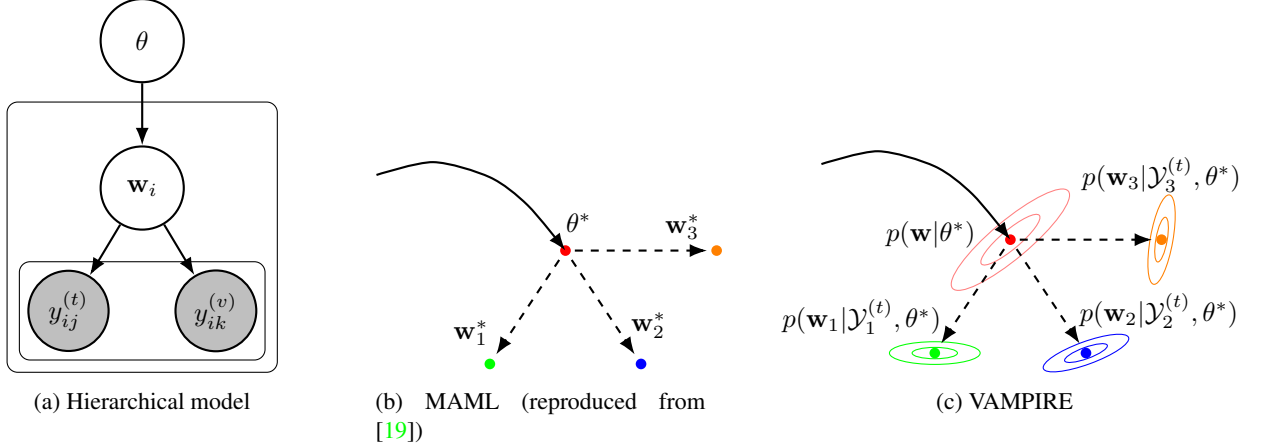


Figure 1: (a) Hierarchical model of the few-shot meta-learning, aiming to learn θ that parameterises prior $p(\mathbf{w}_i; \theta)$, so that given a few data points $y_{ij}^{(t)}$, the model can quickly adapts and accurately predicts $y_{ik}^{(v)}$; (b) and (c) Visualisation between MAML and VAMPIRE, respectively, where VAMPIRE extends the deterministic prior $p(\mathbf{w}_i; \theta)$ and posterior $p(\mathbf{w}_i | \mathcal{Y}_i^{(t)}, \theta)$ in MAML by using probabilistic distributions.

The resulting cost function (excluding the constant term) is often known as the variational free energy. For simplicity, we denote the cost function as

$$\mathcal{L}_i^{(t)}(\lambda_i, \theta) = \text{KL}[q(\mathbf{w}_i; \lambda_i) \| p(\mathbf{w}_i; \theta)] + \mathbb{E}_{q(\mathbf{w}_i; \lambda_i)} \left[-\log p(\mathcal{Y}_i^{(t)} | \mathbf{w}_i) \right]. \quad (9)$$

The first term of the cost function can be considered as a regularisation that penalises the difference between the prior $p(\mathbf{w}_i; \theta)$ and the approximated posterior $q(\mathbf{w}_i; \lambda_i)$, while the second term is referred as data-dependent part or likelihood cost. Exactly minimising the cost function in (9) is computationally challenging, so gradient descent is used with θ as the initialisation of λ_i :

$$\lambda_i \leftarrow \theta - \alpha \nabla_{\lambda_i} \mathcal{L}_i^{(t)}(\lambda_i, \theta), \quad (10)$$

where α is the learning rate.

Given the approximated posterior $q(\mathbf{w}_i; \lambda_i)$ with parameter λ_i updated according to (10), we can calculate and optimise the upper bound in (3) to find a local-optimal meta-parameter θ . This approach leads to the general form of our proposed algorithm, named Variational Agnostic Modelling that Performs Inference for Robust Estimation (VAMPIRE), shown in Algorithm 1.

In Bayesian statistics, the prior $p(\mathbf{w}_i | \theta)$ represents a modelling assumption, and the variational posterior $q(\mathbf{w}_i; \lambda_i)$ is a flexible function that can be adjusted to achieve a good trade-off between performance and complexity. For simplicity, we assume that both $q(\mathbf{w}_i; \lambda_i)$ and $p(\mathbf{w}_i; \theta)$ are Gaussian distributions with diagonal covari-

Algorithm 1 VAMPIRE training

Require: task distribution \mathcal{D}

Require: Hyper-parameters: $T, L_t, L_v, \alpha, \beta$ and γ

- 1: initialise θ
 - 2: **while** θ not converged **do**
 - 3: sample a mini-batch of tasks $\mathcal{T}_i \sim \mathcal{D}, i = 1 : T$
 - 4: **for** each task \mathcal{T}_i **do**
 - 5: $\lambda_i \leftarrow \theta$
 - 6: draw L_t samples $\hat{\mathbf{w}}_i^{(l_t)} \sim q(\mathbf{w}_i; \lambda_i), l_t = 1 : L_t$
 - 7: update: $\lambda_i \leftarrow \lambda_i - \frac{\alpha}{L_t} \nabla_{\lambda_i} \mathcal{L}_i^{(t)}(\lambda_i, \theta)$
 - 8: draw L_v samples $\hat{\mathbf{w}}_i^{(l_v)} \sim q(\mathbf{w}_i; \lambda_i), l_v = 1 : L_v$
 - 9: $\mathcal{L}_i^{(v)}(\mathcal{Y}_i^{(v)}, \theta) = \frac{-1}{L_v} \sum_{l_v=1}^{L_v} \log p(\mathcal{Y}_i^{(v)} | \hat{\mathbf{w}}_i^{(l_v)})$
 - 10: **end for**
 - 11: meta-update: $\theta \leftarrow \theta - \frac{\gamma}{T} \nabla_{\theta} \sum_{i=1}^T \mathcal{L}_i^{(v)}(\mathcal{Y}_i^{(v)}, \theta)$
 - 12: **end while**
-

ance matrices:

$$\begin{cases} p(\mathbf{w}_i; \theta) &= \mathcal{N}[\mathbf{w}_i | \boldsymbol{\mu}_{\theta}, \boldsymbol{\Sigma}_{\theta} = \text{diag}(\boldsymbol{\sigma}_{\theta}^2)] \\ q(\mathbf{w}_i; \lambda_i) &= \mathcal{N}[\mathbf{w}_i | \boldsymbol{\mu}_{\lambda_i}, \boldsymbol{\Sigma}_{\lambda_i} = \text{diag}(\boldsymbol{\sigma}_{\lambda_i}^2)], \end{cases} \quad (11)$$

where $\boldsymbol{\mu}_{\theta}, \boldsymbol{\mu}_{\lambda_i}, \boldsymbol{\sigma}_{\theta}, \boldsymbol{\sigma}_{\lambda_i} \in \mathbb{R}^d$, with d denoting the number of model parameters, and the operator $\text{diag}(\cdot)$ returns a diagonal matrix using the vector in the parameter.

Given the prior $p(\mathbf{w}_i | \theta)$ and the posterior $q(\mathbf{w}_i; \lambda_i)$, we can compute the KL divergence of the cost function shown in (9) by using either Monte Carlo sampling or a closed-form solution. According to [38], sampling model parameters from the approximated posterior $q(\mathbf{w}_i; \lambda_i)$ to compute the KL divergence term and optimise the cost function in (9)

does not perform better or worse than using the closed-form of the KL divergence between two Gaussian distributions. Therefore, we employ the closed-form formula of the KL divergence to speed up the training process.

For numerical stability, we parameterise the standard deviation point-wisely as $\sigma = \exp(\rho)$ when performing gradient update for the standard deviations of model parameters. The meta-parameters $\theta = (\mu_\theta, \exp(\rho_\theta))$ are the initial mean and standard deviation of neural network weights, and the variational parameters $\lambda_i = (\mu_{\lambda_i}, \exp(\rho_{\lambda_i}))$ are the mean and standard deviation of those network weights optimised for task \mathcal{T}_i . We also implement the reparameterisation trick presented in [39] when sampling the network weights from the approximated posterior to compute the expectation of the data log-likelihood in (9):

$$\mathbf{w}_i = \mu_{\lambda_i} + \epsilon \odot \exp(\rho_{\lambda_i}), \quad (12)$$

where $\epsilon \sim \mathcal{N}(0, \mathbf{I}_d)$, and \odot is the element-wise multiplication. Given this direct dependency, the gradients of the cost function $\mathcal{L}_i^{(t)}$ in (9) with respect to λ_i can be derived as:

$$\begin{cases} \nabla_{\mu_{\lambda_i}} \mathcal{L}_i^{(t)} &= \frac{\partial \mathcal{L}_i^{(t)}}{\partial \mathbf{w}_i} + \frac{\partial \mathcal{L}_i^{(t)}}{\partial \mu_{\lambda_i}} \\ \nabla_{\rho_{\lambda_i}} \mathcal{L}_i^{(t)} &= \frac{\partial \mathcal{L}_i^{(t)}}{\partial \mathbf{w}_i} \epsilon \odot \exp(\rho_{\lambda_i}) + \frac{\partial \mathcal{L}_i^{(t)}}{\partial \rho_{\lambda_i}}. \end{cases} \quad (13)$$

After obtaining the variational parameters λ_i in (10), we can apply Monte Carlo approximation by sampling L_v sets of model parameters from the approximated posterior $q(\mathbf{w}_i; \lambda_i)$ to calculate and optimise the upper bound in (3) with regards to the meta-parameters θ .

3.4. Differentiating VAMPIRE and Other Methods in the Literature

VAMPIRE and MAML [19] are fundamentally different because MAML is a deterministic algorithm that employs point estimates on both the prior $p(\mathbf{w}_i; \theta)$ and the task-specific posterior $p(\mathbf{w}_i | \mathcal{Y}_i^{(t)}, \theta)$ (see section 3.2), while VAMPIRE models these distributions in a probabilistically manner. This difference is depicted in Figure 1b and Figure 1c.

VAMPIRE is also different from the ‘‘probabilistic MAML’’ - PLATIPUS [25] in several ways. First, PLATIPUS uses VI to approximate the joint distribution $p(\mathbf{w}_i, \theta | \mathcal{Y}_i^{(t)}, \mathcal{Y}_i^{(v)})$, while VAMPIRE variationally approximates the task-specific posterior $p(\mathbf{w}_i | \mathcal{Y}_i^{(t)}, \theta)$. To handle the complexity of sampling from a joint distribution, PLATIPUS relies on the same point estimate of the task-specific posterior as MAML, as shown in (4). Second, PLATIPUS models the prior $p(\mathbf{w}_i; \mu_\theta, \Sigma_\theta)$ with a fixed variance Σ_θ , while VAMPIRE learns both μ_θ and Σ_θ .

Lastly, when adapting to a task, PLATIPUS requires 2 additional gradient update steps, corresponding to steps 7 and 10 of Algorithm 1 in [25], while VAMPIRE needs only 1 gradient update step as shown in step 7 of Algorithm 1. Hence, VAMPIRE is based on a simpler formulation that does not rely on any point estimate, and it is also more flexible and efficient because it allows all meta-parameters to be learnt while performing less gradient-based steps.

Our proposed algorithm is different from BMAML [20] at the approximation of the task-specific posterior $p(\mathbf{w}_i | \mathcal{Y}_i^{(t)}, \theta)$. BMAML uses SVGD to obtain a closed-form formulation to speed up the gradient-update for the task adaptation. Although SVGD is a non-parametric approach that allows a more flexible variational approximation, its downside is the computational complexity due to kernel matrix, and high memory usage when increasing the number of particles. In contrast, our approach uses a straightforward variational method without any transformation of variables. One advantage of BMAML compared to our method in Algorithm 1 is the use of Chaser Loss, which may be an effective way of preventing overfitting. Nevertheless, in principle, we can also implement the same loss for our proposed algorithm.

VAMPIRE also has many differences compared to [40], although both methods try to solve the same problem. Firstly, the frameworks used in the two methods are different. In [40], PAC-learning was used to derive an upper bound for the multi-task error [40, Eq. 4], and a gradient-based optimisation was carried out to minimise that upper bound. In our work, we employed empirical Bayes, splitting the data set into 2 subsets to cast the multi-task problem into many single tasks, and apply VI on each task. Secondly, the objective functions are dissimilar. While [40] maximises the joint posterior between meta and task-specific parameters $p(\theta, \mathbf{w}_{1:T} | \mathcal{Y}_{1:T})$ [40, Eq. 4 and 19], VAMPIRE minimises the negative conditional likelihood shown in Eq. (1). Lastly, the two algorithms are quite different. In [40], task-specific parameters of λ_i are initialised independently from meta parameters θ , and the optimisation is carried out in a single step as shown in [40, A.4]. In contrast, VAMPIRE uses the meta parameters θ as the initialisation for task-specific parameters λ_i , shown in Eq. (10), and the training is done in 2 optimisation steps as shown in Algorithm 1.

As Amortised Meta-learner [27] is a VI version of [40] (objective function in [27, Eq. (2)] is the same as the one presented in [40, Eq. (23)]), VAMPIRE is different from Amortised Meta-learner at the objective function, and the training procedure.

Compared to VERSA [28], VAMPIRE has different probability distribution parameters to be modelled. VAMPIRE relies on variational distributions to estimate all model parameters of interest, while VERSA is based on an amortisation network to output variational distributions of the last

fully connected layer. The other parameters are point estimates and shared across all tasks. Hence, VAMPIRE is more flexible since it does not need to define which parameters are shared or not shared, nor does it require any additional network. Moreover, being model-agnostic, VAMPIRE is applicable to any machine learning model, while VERSA focuses only on deep neural networks.

4. Experimental Evaluation

The goal of our experiments is to present empirical evaluation of VAMPIRE compared to state-of-art meta-learning approaches. Our experiments include both regression and few-shot classification problems. The experiments are carried out using the training procedure shown in Algorithm 1. All implementations of VAMPIRE use PyTorch [41].

4.1. Regression

We evaluate VAMPIRE using a multi-modal task distribution where half of the data is generated from sinusoidal functions, while the other half is from linear functions [25]. The amplitude and phase of the sinusoids are uniformly sampled from $[0.1, 5]$ and $[0, \pi]$, respectively, while the slope and intercept of the lines are sampled from $[-3, 3]$. Data is generated by uniformly sampling input from $[-5, 5]$, and adding a zero-mean Gaussian noise with a standard deviation of 0.3 to the corresponding labels. The model used is a 3-hidden fully connected neural network with 100 hidden units in each layer. The variational parameters λ_i is estimated by performing 5 gradient updates with learning rate $\alpha = 0.001$. The meta-parameters θ is obtained by using Adam [42] with a fixed step size $\gamma = 0.001$.

The results in Figure 2 show that VAMPIRE can effectively reason which underlying function generates the training data points as the predictions are all sinusoidal or linear. In addition, VAMPIRE is able to vary the prediction variance, especially when there is more uncertainty in the training data. In contrast, due to the deterministic nature, MAML can only output a single value at each data point, and might result in inadequate prediction as shown in the right column of Figure 2.

4.2. Few-shot Classification

The experiments in this sub-section are based on the N -way k -shot learning task, where a meta learner is trained on many related tasks containing N classes and small training sets of k samples for each class (i.e., this is the size of $\mathcal{Y}_i^{(t)}$). We benchmark our results against the state of the art on the data sets Omniglot [8] and mini-ImageNet [16, 23].

Omniglot contains 1623 different handwritten characters from 50 different alphabets, where each one of the characters was drawn online via Amazon’s Mechanical Turk by 20 different people [8]. Omniglot is often split by randomly

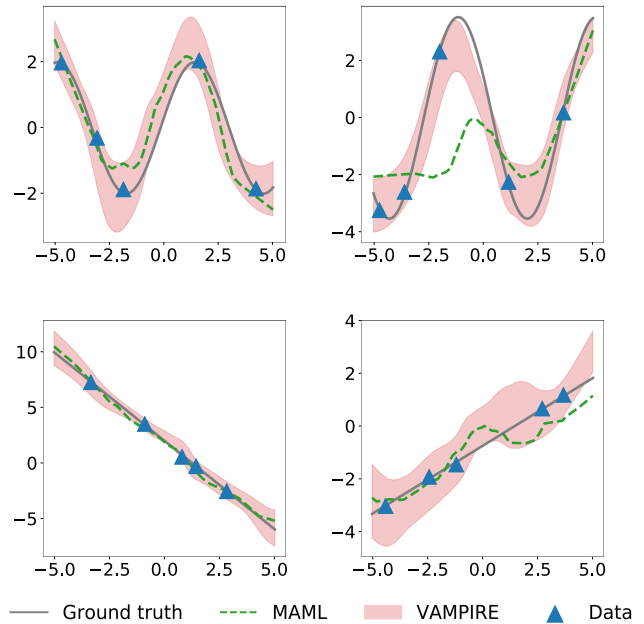


Figure 2: VAMPIRE and MAML are compared in a regression problem when training is based on multi-modal data – half of the tasks are generated from sinusoidal functions, and the other half are from linear functions. The shaded area is the prediction made by VAMPIRE $\pm 1 \times$ standard deviation.

picking 1200 characters for training and the remaining for testing [16, 18, 19]. However, for language character classification, this random split may be unfair since knowing a character of an alphabet may facilitate the learning of other characters in the same alphabet. The original train-test split defined in [8] suggests 30 alphabets for training and 20 alphabets for testing – such split clearly avoids potential information leakage from the training set to the testing set. We run experiments using both splits to compare with state-of-the-art methods and to perform testing without any potential data leakage. As standardly done in the literature, our training includes a data augmentation based on rotating the samples by multiples of 90 degrees, as proposed in [15]. Before performing experiments, all Omniglot images are down-sampled to 28-by-28 pixels to be consistent with the reported works in the meta-learning literature [16, 19, 23].

Mini-ImageNet was proposed in [23] as an evaluation for few-shot learning. It consists of 100 different classes, each having 600 colour images taken from the original ImageNet data set [46]. We use the train-test split reported in [16] that consists of 64 classes for training, 16 for validation, and 20 for testing. Similarly to Omniglot, the examples in mini-ImageNet are pre-processed by down-sampling the images to 84-by-84 pixels to be consistent with previous works in

	5-WAY		20-WAY	
	1-SHOT	5-SHOT	1-SHOT	5-SHOT
OMNIGLOT [8] - ORIGINAL SPLIT, STANDARD 4-LAYER CNN				
MAML	96.68 ± 0.57	98.33 ± 0.22	84.38 ± 0.64	96.32 ± 0.17
VAMPIRE	96.27 ± 0.38	98.77 ± 0.27	86.60 ± 0.24	96.14 ± 0.10
OMNIGLOT [8] - RANDOM SPLIT, STANDARD 4-LAYER CNN				
MATCHING NETS [23]	98.1	98.9	93.8	98.5
PROTOTYPICAL NETS [18] ²	98.8	99.7	96.0	98.9
MAML [19]	98.7 ± 0.4	99.9 ± 0.1	95.8 ± 0.3	98.9 ± 0.2
VAMPIRE	98.43 ± 0.19	99.56 ± 0.08	93.20 ± 0.28	98.52 ± 0.13
OMNIGLOT [8] - RANDOM SPLIT, NON-STANDARD CNNs				
SIAMESE NETS [43]	97.3	98.4	88.2	97.0
NEURAL STATISTICIAN [30]	98.1	99.5	93.2	98.1
MEMORY MODULE [44]	98.4	99.6	95.0	98.6
RELATION NETS [45]	99.6 ± 0.2	99.8 ± 0.1	97.6 ± 0.2	99.1 ± 0.1
VERSA [28]	99.70 ± 0.20	99.75 ± 0.13	97.66 ± 0.29	98.77 ± 0.18

Table 1: Few-shot classification accuracy (in percentage) on Omniglot, tested on 1000 tasks and reported with 95% confidence intervals. The results of VAMPIRE are competitive to the state-of-the-art baselines which are carried out on a standard 4-convolution-layer neural networks. The top of the table contains methods trained on the original split defined in [8], while the middle part contains methods using a standard 4-layer CNN trained on random train-test split. The bottom part presents results of different methods using different network architectures, or requiring external modules and additional parameters trained on random split. Note that the Omniglot results on random split cannot be fairly compared.

the literature.

We use the same network architecture of state-of-the-art methods [16, 19, 23]. The network consists of 4 hidden convolution modules, each containing 64 3-by-3 filters, followed by batch normalisation [47], ReLU activation, and a 2-by-2 strided convolution. For the mini-ImageNet, the strided convolution is replaced by a 2-by-2 max-pooling layer, and only 32 filters are used on each convolution layer to avoid over-fitting as done in [16, 19]. The output size of the last hidden module is, therefore, 64 for Omniglot and 800 for mini-ImageNet. These units are then fully-connected to the output layer followed by a softmax activation. Please refer to Appendices for detailed description on the training and the hyperparameters used.

The N -way k -shot classification accuracy measured on Omniglot and mini-ImageNet data sets are shown in Tables 1 and 2, respectively. Although our goal is to compare algorithms by using the standard 4-layer CNN, we also include the state-of-the-art methods that employ much deeper networks with various architectures to provide a broad view of the few-shot image classification. Overall, the results of VAMPIRE are competitive to the state-of-the-art methods that use the same network architecture [16, 19, 23].

On Omniglot, our results on a random train-test split are competitive in most scenarios. Our proposed method outperforms some previous works in few-shot learning, such as

siamese networks [43], matching networks [23] and memory models [44], although they are designed with a focus on few-shot classification. Our result on the 20-way 1-shot is slightly lower than prototypical networks [18] and VERSA [28], but prototypical networks need more classes (higher “way”) per training episode to obtain advantageous results and VERSA requires an additional amortised networks to learn the variational distributions. Our results are also slightly lower than MAML, potentially due to the difference of train-test split. To obtain a fair comparison, we run the public code provided by MAML’s authors, and measure its accuracy on the original split suggested in [8]. Using this split, VAMPIRE achieves competitive performance, and outperforms MAML in some cases.

On mini-ImageNet, VAMPIRE outperforms all reported methods that use the standard 4-layer CNN architecture on the 1-shot tests, while being competitive on the 5-shot episodes. Prototypical Networks achieve a higher accuracy on the 5-shot tests due to, again, the use of extra classes during training. Although our work does not aim to achieve the state-of-the-art results in few-shot learning, we also run an experiment with input as features extracted by a residual network that was pre-trained on data and classes from training meta-set [22, Sect. 4.2.2], and present the results at the bottom part of Table 2. Compared to some recent methods such as TADAM [48] and LEO [22], our results achieve the current state-of-the-art results in 1-shot, and are competitive

²Trained with 60-way episodes.

	5-WAY	
	1-SHOT	5-SHOT
MINI-IMAGENET [16] - STANDARD 4-BLOCK CNN		
MATCHING NETS [23]	43.56 \pm 0.84	55.31 \pm 0.73
META-LEARNER LSTM [16]	43.44 \pm 0.77	60.60 \pm 0.71
MAML [19]	48.70 \pm 1.84	63.15 \pm 0.91
PROTOTYPICAL NETS [18] ³	49.42 \pm 0.78	68.20 \pm 0.66
LLAMA [24]	49.40 \pm 1.83	-
PLATIPUS [25]	50.13 \pm 1.86	-
AMORTISED ML [27]	45.00 \pm 0.60	-
VAMPIRE	51.54 \pm 0.74	64.31 \pm 0.74
MINI-IMAGENET [16] - NON-STANDARD CNN		
RELATION NETS [45]	50.44 \pm 0.82	65.32 \pm 0.70
VERSA [28]	53.40 \pm 1.82	67.37 \pm 0.86
SNAIL [49]	55.71 \pm 0.99	68.88 \pm 0.92
ADARESNET [50]	56.88 \pm 0.62	71.94 \pm 0.57
TADAM [48]	58.5 \pm 0.30	76.7 \pm 0.30
LEO [22]	61.76 \pm 0.08	77.59 \pm 0.12
VAMPIRE	62.16 \pm 0.24	76.72 \pm 0.37

Table 2: The few-shot classification accuracy results (in percentage) of VAMPIRE averaged over 600 mini-ImageNet tasks are competitive to the state-of-the-art methods. For a fair comparison, we decouple the effect of network architecture with the ones on top, including VAMPIRE, using the standard 4-block convolution network, while the bottom part uses extra parameters, deeper network architectures or different training settings.

in 5-shot. Note that the results in the bottom part of Table 2 are not directly comparable since the network architecture used and the training setting vary in each method.

To evaluate the predictive uncertainty of the models, we show in Figures 3a-3d the reliability diagrams [51] across many unseen tasks tested to compare different models. A perfectly calibrated model will have its values overlapped with the identity function $y = x$, indicating that the probability associated with the label prediction is the same as the true probability. Here, only a few methods are compared because they have similar network architectures, and the training does not require any additional parameters as VERSA or extra classes as Prototypical Networks. According to the reliability graphs, the model trained with VAMPIRE shows a much better calibration than the ones trained with MAML and PLATIPUS, while being competitive to Amortised Meta-learner. To further evaluate, we compute the expected calibration error (ECE) and maximum calibration error (MCE) [51] of each models trained with these methods. The results plotted in Figure 3e show that the model trained with VAMPIRE has smaller ECE and MCE compared to MAML and PLATIPUS. VAMPIRE has a lower ECE and a

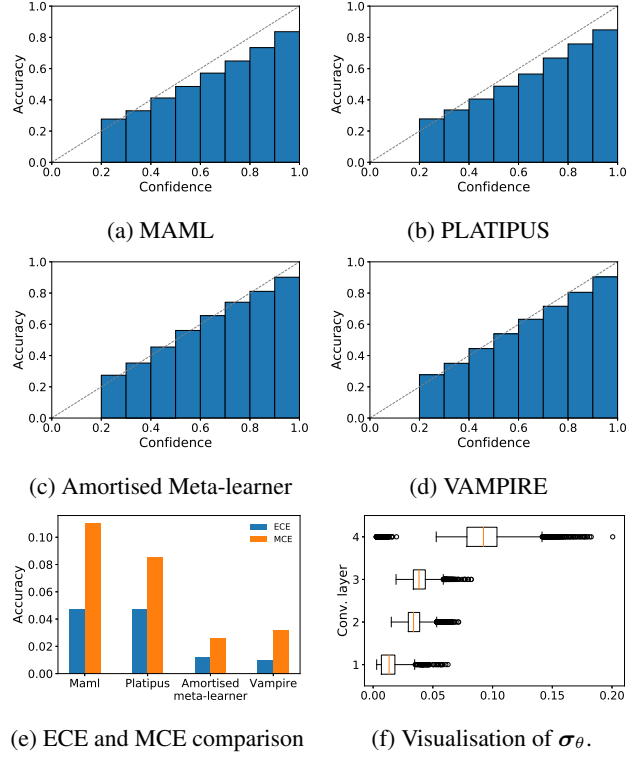


Figure 3: Uncertainty evaluation between different meta-learning methods using: (a)-(d) reliability diagrams, and (e) Expected calibration error (ECE) and maximum calibration error (MCE). In addition, standard deviations of meta-parameters σ_θ across convolutional layers plotted in (f) shows no distribution collapse when modelling network weight uncertainty using VAMPIRE. The evaluation is carried out on 5-way 1-shot unseen tasks sampled from mini-ImageNet dataset.

competitive MCE compared to Amortised Meta-learner, but notice that Amortised Meta-learner has a worse classification result than VAMPIRE, as shown in Table 2. In addition, the standard deviations of meta-parameters σ_θ trained with VAMPIRE in Figure 3f shows no distribution collapse when modelling the uncertainty of meta-parameters.

5. Conclusion

We introduce and formulate a new Bayesian algorithm used for few-shot meta-learning. The proposed algorithm, VAMPIRE, employs variational inference to optimise a well-defined cost function to learn a distribution of model parameters. The uncertainty, in the form of the learnt distribution, can introduce more variability into the decision made by the model, resulting in well-calibrated and highly-accurate prediction. The algorithm can be combined with

³Trained with 30-way episodes for 1-shot classification and 20-way episodes for 5-shot classification

different models that are trainable with gradient-based optimisation, and is applicable in regression and classification. We demonstrate that the algorithm can make reasonable predictions about unseen data in a multi-modal 5-shot learning regression problem, and achieve state-of-the-art calibration and classification results with only 1 or 5 training examples per class on public image data sets.

References

- [1] G. Hinton, L. Deng, D. Yu, G. E. Dahl, A.-r. Mohamed, N. Jaitly, A. Senior, V. Vanhoucke, P. Nguyen, T. N. Sainath, *et al.*, “Deep neural networks for acoustic modeling in speech recognition: The shared views of four research groups,” *IEEE Signal processing magazine*, vol. 29, no. 6, pp. 82–97, 2012.
- [2] A. Graves, A.-r. Mohamed, and G. Hinton, “Speech recognition with deep recurrent neural networks,” in *IEEE International Conference on Acoustics, Speech and Signal Processing (ICASSP), 2013*, IEEE, 2013, pp. 6645–6649.
- [3] A. Krizhevsky, I. Sutskever, and G. E. Hinton, “Imagenet classification with deep convolutional neural networks,” in *Advances in neural information processing systems*, 2012, pp. 1097–1105.
- [4] K. Simonyan and A. Zisserman, “Very deep convolutional networks for large-scale image recognition,” in *International Conference on Learning Representations*, 2015.
- [5] M. Havaei, A. Davy, D. Warde-Farley, A. Biard, A. Courville, Y. Bengio, C. Pal, P.-M. Jodoin, and H. Larochelle, “Brain tumor segmentation with deep neural networks,” *Medical image analysis*, vol. 35, pp. 18–31, 2017.
- [6] X. Glorot and Y. Bengio, “Understanding the difficulty of training deep feedforward neural networks,” in *Proceedings of the thirteenth international conference on artificial intelligence and statistics*, 2010, pp. 249–256.
- [7] M. T. Rosenstein, Z. Marx, L. P. Kaelbling, and T. G. Dietterich, “To transfer or not to transfer,” in *NIPS 2005 workshop on transfer learning*, vol. 898, 2005, pp. 1–4.
- [8] B. M. Lake, R. Salakhutdinov, and J. B. Tenenbaum, “Human-level concept learning through probabilistic program induction,” *Science*, vol. 350, no. 6266, pp. 1332–1338, 2015.
- [9] R. Caruana, “Multitask learning,” *Machine learning*, vol. 28, no. 1, pp. 41–75, 1997.
- [10] J. S. Bridle and S. J. Cox, “Recnorm: Simultaneous normalisation and classification applied to speech recognition,” in *Advances in Neural Information Processing Systems*, 1991, pp. 234–240.
- [11] S. Ben-David, J. Blitzer, K. Crammer, A. Kulesza, F. Pereira, and J. W. Vaughan, “A theory of learning from different domains,” *Machine learning*, vol. 79, no. 1-2, pp. 151–175, 2010.
- [12] L. Fei-Fei, R. Fergus, and P. Perona, “One-shot learning of object categories,” *IEEE transactions on pattern analysis and machine intelligence*, vol. 28, no. 4, pp. 594–611, 2006.
- [13] J. Schmidhuber, “Evolutionary principles in self-referential learning (on learning how to learn: The meta-meta-... hook),” Diploma thesis, Technische Universität München, 1987.
- [14] S. Thrun and L. Pratt, *Learning to learn*. Springer Science & Business Media, 1998.
- [15] A. Santoro, S. Bartunov, M. Botvinick, D. Wierstra, and T. Lillicrap, “Meta-learning with memory-augmented neural networks,” in *International Conference on Machine Learning*, 2016, pp. 1842–1850.
- [16] S. Ravi and H. Larochelle, “Optimization as a model for few-shot learning,” in *International Conference on Learning Representations*, 2017.
- [17] T. Munkhdalai and H. Yu, “Meta networks,” in *International Conference on Machine Learning*, 2017.
- [18] J. Snell, K. Swersky, and R. Zemel, “Prototypical networks for few-shot learning,” in *Advances in Neural Information Processing Systems*, 2017, pp. 4077–4087.
- [19] C. Finn, P. Abbeel, and S. Levine, “Model-agnostic meta-learning for fast adaptation of deep networks,” in *International Conference on Machine Learning*, 2017, pp. 1126–1135.
- [20] J. Yoon, T. Kim, O. Dia, S. Kim, Y. Bengio, and S. Ahn, “Bayesian model-agnostic meta-learning,” in *Advances in Neural Information Processing Systems 31*, 2018, pp. 7343–7353.
- [21] R. Zhang, T. Che, Z. Ghahramani, Y. Bengio, and Y. Song, “Metagan: An adversarial approach to few-shot learning,” in *Advances in Neural Information Processing Systems 31*, 2018, pp. 2371–2380.
- [22] A. A. Rusu, D. Rao, J. Sygnowski, O. Vinyals, R. Pascanu, S. Osindero, and R. Hadsell, “Meta-learning with latent embedding optimization,” in *International Conference on Learning Representations*, 2019.

- [23] O. Vinyals, C. Blundell, T. Lillicrap, D. Wierstra, *et al.*, “Matching networks for one shot learning,” in *Advances in Neural Information Processing Systems*, 2016, pp. 3630–3638.
- [24] E. Grant, C. Finn, S. Levine, T. Darrell, and T. Griffiths, “Recasting gradient-based meta-learning as hierarchical bayes,” in *International Conference on Learning Representations*, 2018.
- [25] C. Finn, K. Xu, and S. Levine, “Probabilistic model-agnostic meta-learning,” in *Conference on Neural Information Processing Systems*, 2018, pp. 9537–9548.
- [26] D. K. Naik and R. Mammone, “Meta-neural networks that learn by learning,” in *International Joint Conference on Neural Networks*, IEEE, vol. 1, 1992, pp. 437–442.
- [27] S. Ravi and A. Beatson, “Amortized bayesian meta-learning,” in *International Conference on Learning Representations*, 2019.
- [28] J. Gordon, J. Bronskill, M. Bauer, S. Nowozin, and R. Turner, “Meta-learning probabilistic inference for prediction,” in *International Conference on Learning Representations*, 2019.
- [29] M. Garnelo, J. Schwarz, D. Rosenbaum, F. Viola, D. J. Rezende, S. Eslami, and Y. W. Teh, “Neural processes,” in *ICML workshop on Theoretical Foundations and Applications of Deep Generative Models*, 2018.
- [30] H. Edwards and A. Storkey, “Towards a neural statistician,” in *International Conference on Learning Representation*, 2017.
- [31] A. M. Saxe, J. L. McClelland, and S. Ganguli, “Exact solutions to the nonlinear dynamics of learning in deep linear neural networks,” in *International Conference on Learning Representation*, 2014.
- [32] J. Kirkpatrick, R. Pascanu, N. Rabinowitz, J. Veness, G. Desjardins, A. A. Rusu, K. Milan, J. Quan, T. Ramalho, A. Grabska-Barwinska, *et al.*, “Overcoming catastrophic forgetting in neural networks,” *Proceedings of the national academy of sciences*, p. 201 611 835, 2017.
- [33] P. Krähenbühl, C. Doersch, J. Donahue, and T. Darrell, “Data-dependent initializations of convolutional neural networks,” in *International Conference on Learning Representation*, 2016.
- [34] T. Salimans and D. P. Kingma, “Weight normalization: A simple reparameterization to accelerate training of deep neural networks,” in *Advances in Neural Information Processing Systems*, 2016, pp. 901–909.
- [35] M. Husken and C. Goerick, “Fast learning for problem classes using knowledge based network initialization,” in *Proceedings of the IEEE-INNS-ENNS International Joint Conference on Neural Networks*, IEEE, vol. 6, 2000, pp. 619–624.
- [36] D. Maclaurin, D. Duvenaud, and R. Adams, “Gradient-based hyperparameter optimization through reversible learning,” in *International Conference on Machine Learning*, 2015, pp. 2113–2122.
- [37] J. Baxter, “A model of inductive bias learning,” *Journal of Artificial Intelligence Research*, vol. 12, pp. 149–198, 2000.
- [38] C. Blundell, J. Cornebise, K. Kavukcuoglu, and D. Wierstra, “Weight uncertainty in neural networks,” in *International Conference on Machine Learning*, 2015, pp. 1613–1622.
- [39] D. P. Kingma and M. Welling, “Auto-encoding variational bayes,” in *International Conference on Learning Representations*, 2014.
- [40] R. Amit and R. Meir, “Meta-learning by adjusting priors based on extended PAC-Bayes theory,” in *International Conference on Machine Learning*, 2018, pp. 205–214.
- [41] A. Paszke, S. Gross, S. Chintala, G. Chanan, E. Yang, Z. DeVito, Z. Lin, A. Desmaison, L. Antiga, and A. Lerer, “Automatic differentiation in pytorch,” in *NIPS Workshop on Automatic Differentiation*, 2017.
- [42] D. P. Kingma and J. Ba, “Adam: A method for stochastic optimization,” in *International Conference on Learning Representations*, 2015.
- [43] G. Koch, R. Zemel, and R. Salakhutdinov, “Siamese neural networks for one-shot image recognition,” in *ICML Deep Learning Workshop*, vol. 2, 2015.
- [44] Ł. Kaiser, O. Nachum, A. Roy, and S. Bengio, “Learning to remember rare events,” in *International Conference on Learning Representations*, 2017.
- [45] F. Sung, Y. Yang, L. Zhang, T. Xiang, P. H. Torr, and T. M. Hospedales, “Learning to compare: Relation network for few-shot learning,” in *Conference on Computer Vision and Pattern Recognition*, 2018.
- [46] J. Deng, W. Dong, R. Socher, L.-J. Li, K. Li, and L. Fei-Fei, “ImageNet: A Large-Scale Hierarchical Image Database,” in *Conference on Computer Vision and Pattern Recognition*, 2009.
- [47] S. Ioffe and C. Szegedy, “Batch normalization: Accelerating deep network training by reducing internal covariate shift,” in *International Conference on Machine Learning*, 2015, pp. 448–456.

- [48] B. N. Oreshkin, A. Lacoste, and P. Rodriguez, “Tadam: Task dependent adaptive metric for improved few-shot learning,” in *Conference on Neural Information Processing Systems*, 2018, pp. 719–729.
- [49] N. Mishra, M. Rohaninejad, X. Chen, and P. Abbeel, “A simple neural attentive meta-learner,” in *International Conference on Learning Representations*, 2018.
- [50] T. Munkhdalai, X. Yuan, S. Mehri, and A. Trischler, “Rapid adaptation with conditionally shifted neurons,” in *International Conference on Machine Learning*, 2018, pp. 3661–3670.
- [51] C. Guo, G. Pleiss, Y. Sun, and K. Q. Weinberger, “On calibration of modern neural networks,” in *International Conference on Machine Learning*, 2017.

A. Training configuration

This section describes the detailed setup to train and validate the few-shot learning on Omniglot and mini-ImageNet presented in Sec. 4.2. Following the notation used in Sec. 3.1, each task or episode i has N classes, where the support set $\mathcal{Y}_i^{(t)}$ has k samples per class, and the query set $\mathcal{Y}_i^{(v)}$ has 15 samples per class. This is to be consistent with the previous works in the literature [16, 19]. The training is carried out by using Adam to minimise the cross-entropy loss of the softmax output. The learning rate of the meta-parameters θ is set to be $\gamma = 10^{-3}$ across all trainings, and decayed by a factor of 0.99 after every 10,000 tasks. Other hyperparameters used are specified in Tab. 3. We select the number of ensemble models L_t and L_v to fit into the memory of one Nvidia 1080 Ti GPU. Higher values of L_t and L_v are desirable to achieve a better Monte Carlo approximation.

DESCRIPTION	NOTATION	OMNIGLOT		MINI-IMAGENET
		5-WAY	20-WAY	5-WAY
NUMBER TASKS PER META-UPDATE	T	32	16	2
NUMBER OF ENSEMBLE MODELS (TRAIN)	L_t (TRAIN)	1	1	10
NUMBER OF ENSEMBLE MODELS (TRAIN)	L_v (TRAIN)	1	1	10
NUMBER OF ENSEMBLE MODELS (TEST)	L_t (TEST)	10	10	10
NUMBER OF ENSEMBLE MODELS (TEST)	L_v (TEST)	10	10	10
LEARNING RATE FOR ϕ_i	α	0.1	0.1	0.01
LEARNING RATE FOR θ	γ	10^{-3}	10^{-3}	10^{-3}
NUMBER OF INNER GRADIENT UPDATES		5	5	5
L2 REGULARISATION FOR μ_θ		10^{-5}	10^{-5}	10^{-5}
L2 REGULARISATION FOR ρ_θ		0	0	10^{-6}

Table 3: Hyperparameters used in the few-shot classification presented in Sec. 4.

We also note that the training of Prototypical Networks [18] is slightly different from the conventional training on N -way k -shot classification. Instead of using the same number of ways (or classes), Prototypical Networks is trained on a higher number of ways to achieve good results. Prototypical Networks require 60 classes for training on the Omniglot, while 30 classes for 1-shot classification and 20 classes for 5-shot classification on mini-ImageNet. According to [45], when being trained with 5-way classification on mini-ImageNet, the performance of Prototypical Networks for the 1-shot setting drops from $49.42 \pm 0.78\%$ to $46.14 \pm 0.77\%$. This is much lower than our reported value using VAMPIRE. To fairly compare, we re-implement the Prototypical Networks. We firstly train and test the performance of the replicated networks using the proposed setting in [18] to assure that our implementation is exact. We then train and validate the performance on the conventional 5-way classification. As shown in Table 4, VAMPIRE outperforms Prototypical Networks when using the same number of classes for train and test on the 1-shot and 5-shot classification on mini-ImageNet dataset.

	SETTING	5-WAY 1-SHOT	5-WAY 5-SHOT
PROTOTYPICAL NETS	REPORTED [18]	49.42 ± 0.78	68.20 ± 0.66
	RE-IMPLEMENTATION	49.13 ± 0.77	66.97 ± 0.72
	5-CLASS	46.75 ± 0.74	64.28 ± 0.69
VAMPIRE	5-CLASS	51.54 ± 0.74	64.31 ± 0.74

Table 4: Compare the accuracy predicted by Prototypical Network (reported and re-implementation) and VAMPIRE on mini-ImageNet dataset.

B. Re-scale KL divergence

The closed-form formula of the KL divergence between two Gaussian distributions can be presented as

$$\text{KL}[\mathcal{N}(\mu_1, \Sigma_1) \parallel \mathcal{N}(\mu_2, \Sigma_2)] = \frac{1}{2} \left[\text{tr}(\Sigma_2^{-1} \Sigma_1) + (\mu_2 - \mu_1)^T \Sigma_2^{-1} (\mu_2 - \mu_1) + \ln \frac{\det(\Sigma_2)}{\det(\Sigma_{\phi_i})} - D \right]. \quad (14)$$

The non-negative property of KL divergence leads to:

$$\begin{aligned} \text{tr}(\Sigma_2^{-1}\Sigma_1) + (\mu_2 - \mu_1)^T \Sigma_2^{-1} (\mu_2 - \mu_1) + \ln \frac{\det(\Sigma_2)}{\det(\Sigma_{\phi_i})} - D &\geq 0 \\ \Rightarrow \text{tr}(\Sigma_2^{-1}\Sigma_1) + (\mu_2 - \mu_1)^T \Sigma_2^{-1} (\mu_2 - \mu_1) + \ln \frac{\det(\Sigma_2)}{\det(\Sigma_{\phi_i})} &\geq D. \end{aligned} \quad (15)$$

Our term of interest is on the left hand side of (15) because the gradient of this term will be used to minimise the variational free energy shown in (9). Given the result in (15), the term of interest is larger than D —the number of network weights. Thus, the more complex the network, the larger this term. To balance the operating scale between the likelihood loss and the KL term in (9), we re-scale the KL divergence in equation (14) by a factor β that is inversely proportional to D . This scales down the lower bound of the left hand side term in (15) from D to a constant. Throughout this paper, we select

$$\beta = \frac{2}{D} \quad (16)$$

for all of our implementations presented in Sect. 4.